The Journal of Chemical Physics

Microscopic models of mode-coupling theory: The F_{12} scenario

Cite as: J. Chem. Phys. **137**, 084501 (2012); https://doi.org/10.1063/1.4746695
Submitted: 27 June 2012 . Accepted: 03 August 2012 . Published Online: 22 August 2012

Jeferson J. Arenzon, and Mauro Sellitto

AIP Publishing

Microscopic models of mode-coupling theory: The F_{12} scenario

Jeferson J. Arenzon[1] and Mauro Sellitto[2]
[1]*Instituto de Física, Universidade Federal do Rio Grande do Sul, CP 15051, 91501-970 Porto Alegre RS, Brazil and LPTHE, Université Pierre et Marie Curie-Paris VI, 4 Place Jussieu, FR-75252 Paris Cedex 05, France*
[2]*Department of Information Engineering, Second University of Naples, I-81031 Aversa (CE), Italy*

(Received 27 June 2012; accepted 3 August 2012; published online 22 August 2012)

We provide extended evidence that mode-coupling theory (MCT) of supercooled liquids for the F_{12} schematic model admits a microscopic realization based on facilitated spin models with tunable facilitation. Depending on the facilitation strength, one observes two distinct dynamical glass transition lines—continuous and discontinuous—merging at a dynamical tricritical-like point with critical decay exponents consistently related by MCT predictions. The mechanisms of dynamical arrest can be naturally interpreted in geometrical terms: the discontinuous and continuous transitions correspond to bootstrap and standard percolation processes, in which the incipient spanning cluster of frozen spins forms either a compact or a fractal structure, respectively. Our cooperative dynamical facilitation picture of glassy behavior is complementary to the one based on disordered systems and can account for higher-order singularity scenarios in the absence of a finite temperature thermodynamic glass transition. We briefly comment on the relevance of our results to finite spatial dimensions and to the F_{13} schematic model. © *2012 American Institute of Physics*. [http://dx.doi.org/10.1063/1.4746695]

I. INTRODUCTION

The glassy state of matter remains an active area of research despite decades of study. From a theoretical viewpoint, the most fundamental issue concerns the very nature of the vitrification process, that is whether the amorphous state represents a genuine thermodynamic phase or rather a purely dynamical accident. It is well known that the issue is made especially difficult by the lack of a suitable observable allowing the unambiguous identification of the elusive *amorphous order*, and the exceedingly long equilibration times involved in experiments and simulations. The situation is further complicated by the fact that theoretical modelling of glassy systems has made clear that slow relaxation phenomena are ubiquitous and may result from very distinct microscopic mechanisms.[1] Thus, it may appear rather unlikely that a single theoretical framework encompasses the large variety of behaviors observed in glassy materials. For this reason, one is often focused on the attempt to predict those features that are thought to be universal in a minimal setting, which is the basic philosophy we adopt here.

Mode-coupling theory (MCT), is considered by many the most comprehensive first-principle approach to the dynamics of supercooled liquids (for reviews, see Refs. 2–5). Despite some limitations, it has been much successful in predicting peculiar higher-order singularities which have been confirmed by experiments and computer simulations.[6–14] A key tenet of MCT is that the glass transition is a purely *dynamical* phenomenon unrelated to any thermodynamic singularity.[15–17] This prediction is rather puzzling from a statistical mechanics point of view because diverging relaxation time-scales are typically associated with diverging lengthscales,[18] and the latter are a consequence of a thermodynamical phase transition, as clearly exemplified by traditional critical phenomena. It has been argued that this unusual situation stems from uncontrolled approximations, which crucially miss thermally activated hopping processes responsible for low-temperature equilibration. Therefore, the dynamical nature of the glass transition singularity has been much debated since its first appearance[19,20] and much work has been devoted to clarify the status of MCT.[21–31]

Fruitful developments in the dynamics of mean-field disordered systems have subsequently shown the intimate connection of some spin-glass models with MCT and led to the formulation of the so-called random first-order transition (RFOT) approach.[21–23] The most important ingredient brought about into the discussion is the existence of an extra *thermodynamic* glass phase at a Kauzmann temperature T_K below the dynamical glass transition predicted by MCT. This has immediately suggested that while the dynamical transition is an artifact of mean-field approximation (and therefore doomed to disappear in real systems), genuine glassy behavior would be a more profound reflection of an underlying non-trivial Gibbs measure corresponding to a one-step replica-symmetry breaking spin-glass phase. Such developments have been generalized in several ways and have led to a low-temperature extension of MCT to off-equilibrium situations, revealing new interesting features such as aging phenomena[32–35] and effective temperature.[36,37]

The thermodynamic RFOT perspective is in apparent conflict with a different line of thought inspired by facilitated (or kinetically constrained) models first introduced by Fredrickson and Andersen[38] (see Ref. 39 for a review). These models have a trivial thermodynamics, and so their glassy behavior has a purely dynamical origin by construction. For this reason, they appear to be at odds with any thermodynamic perspective on the glass transition problem. Moreover, since the simplest (so-called non-cooperative) version of such systems does not have neither a thermodynamic nor a

dynamical transition, the facilitation approach also appears to be inconsistent with MCT. Therefore, the notion of dynamical facilitation seems to provide an alternative way to the glass formation quite in contrast to the MCT and RFOT approach (a viewpoint advocated, e.g., in Ref. 40). It has long been noticed, however, that several peculiar features of MCT and RFOT are also present in facilitated and kinetically constrained systems.[41–43] In fact, we have recently shown that one can construct a class of facilitated spin systems that actually reproduces the two most relevant MCT scenarios.[44,45] This means that the dynamic facilitation approach on one hand, and the MCT and RFOT scenario on the other, should not be considered as alternative but rather as complementary representations of glassy dynamics. Our statement is consistent with recent results showing that, in a specific case, there is an exact mapping between facilitated and disordered spin systems.[46]

In this paper we present detailed numerical results supporting the idea that cooperative facilitated systems provide a microscopic realization of MCT including higher-order bifurcation singularity. The rest of the paper is organized as follows. To set the stage, in Sec. II, we briefly review the basic predictions of MCT approach to glass transition. In Sec. III, we introduce facilitated spin systems and recall their connections to the bootstrap percolation problem on a Bethe lattice. In Sec. IV we define the model we study in this paper and report the exact results for the phase diagram and the arrested part of correlations. Numerical simulation for the relaxation time and the critical decay law exponents are presented and compared with MCT predictions in Sec. V. Finally, in Sec. VI we present the conclusions and possible directions of future works including a brief discussion on the possible relevance of our results to finite spatial dimension and to the F_{13} schematic model. Some technical calculations are reported in the Appendix.

II. MODE-COUPLING THEORY: THE F_{12} SCENARIO

A comprehensive description of MCT can be found in Ref. 3. Here, we outline only those aspects which are pertinent to the present work and that are useful for comparison with our theoretical and simulation results. In particular, since we focus on schematic models we shall disregard the wavevector dependence of the relevant physical quantities. In the MCT, the microscopic system dynamics is projected, through the Zwanzig-Mori formalism, on a set of observables which is thought to be physically relevant, namely the local density fluctuations, $\delta\rho(t)$. The correlator of these quantity $\phi(t) = \langle \delta\rho(t)\delta\rho(0)\rangle / \langle |\delta\rho|^2\rangle$ is shown to exactly obey the evolution equation:

$$\phi(t) + \tau_0 \dot{\phi}(t) + \int_0^t m(t-s)\,\dot{\phi}(s)\,\mathrm{d}s = 0, \qquad (1)$$

where τ_0 is the characteristic microscopic timescale of the system and we assume, for simplicity, overdamped local motion appropriate, e.g., to hard-sphere colloids (for molecular liquids one should add an inertial term). The memory kernel $m(t-s)$ takes into account the retarded friction effect which arises from the caging of a particle by its neighbors. It is controlled by the static structure factor $S(q) = (1/N)\langle |\delta\rho|^2\rangle$ and does not involve any thermodynamic singularity. In the dilute limit the memory function is negligible and the relaxation is exponential. At high-density or low-temperature, the memory kernel cause a viscosity increase through a feedback mechanism that eventually leads to the structural arrest of fluctuations. For a general system, the explicit expression of $m(t-s)$ is rather complicated, and in order to obtain quantitative predictions, one is forced to introduce some approximations. In schematic models the memory function is approximated by a low order polynomial of correlators, with coupling constants that depend solely on $S(q)$. A key quantity in describing the liquid-glass transition is the so-called nonergodicity parameter (also known as Edwards-Anderson parameter in the spin-glass literature), that is the long-time limit of the correlator,

$$\Phi = \lim_{t\to\infty} \phi(t). \qquad (2)$$

In the fluid state, the system is ergodic and $\phi(t)$ decays to zero with time, $\Phi = 0$. When Φ is finite the system is unable to fully relax, its dynamical is arrested and the liquid becomes a glass. For schematic models one can easily derive the liquid-glass phase diagram. Taking the long-time limit of Eq. (1), one obtains the bifurcation equation:

$$\frac{\Phi}{1-\Phi} = m\,[\Phi]\,, \qquad (3)$$

whose solutions possibly give different types of ergodic-nonergodic transitions. Of interest here is the so-called F_{12} schematic model which is defined by the memory function

$$m\,[\phi(t)] = v_1\phi(t) + v_2\phi^2(t), \qquad (4)$$

where v_1, v_2 are the coupling parameters controlling the system state. In this case, by solving the bifurcation equation one finds a *discontinuous* liquid-glass transition line, $v_1^c = \sqrt{4v_2} - v_2$ with $v_2 \in [1,4]$, at which Φ jumps from zero to a finite value Φ_c, with a square-root singularity, $\Phi - \Phi_c \sim \epsilon^{1/2}$, where ϵ is the distance from the transition line. For $v_2 \in [0,1]$ one finds a *continuous* liquid-glass transition, $v_1^c = 1$, across which Φ smoothly departs from zero in a linear fashion, $\Phi \sim \epsilon$.

On the liquid side of the relaxation dynamics, MCT makes several specific predictions. Near the discontinuous transition line, the relaxation has a peculiar two-step form. The approach and departure from the critical plateau at Φ_c, respectively, defining the β and α relaxation regimes, are described by the so-called critical decay laws:

$$|\phi(t) - \Phi_c| \sim \begin{cases} (t/\tau_\beta)^{-a}, & \beta\text{-regime;} \\ (t/\tau)^{-b}, & \alpha\text{-regime.} \end{cases} \qquad (5)$$

The two characteristic times τ and τ_β, respectively, associated with the α and β regimes, increase as power-laws near the critical line:

$$\tau \sim \epsilon^{-\gamma}, \qquad \tau_\beta \sim \epsilon^{-1/2a}. \qquad (6)$$

The exponents a, b, and γ are not independent but obey the relations:

$$\lambda = \frac{\Gamma^2(1-a)}{\Gamma(1-2a)} = \frac{\Gamma^2(1+b)}{\Gamma(1+2b)}, \qquad \gamma = \frac{1}{2a} + \frac{1}{2b}, \qquad (7)$$

where Γ is the Euler's gamma function. The correlator presents universal scaling (the so-called time-temperature superposition principle) in the late α-regime: rescaling time by the structural relaxation time τ, one obtains that data for correlator near the critical line can be collapsed onto a single master function.

Near the continuous transition line there is no α-regime and one finds a single step relaxation with a weak-long time tail described by the critical decay law of the β-regime, i.e., the first of Eq. (5) with $\Phi_c = 0$ remains valid. However, the exponent characterizing the relaxation time is twice that of the discontinuous transition:

$$\tau_\beta \sim \epsilon^{-1/a}. \tag{8}$$

It is important to notice that the exponent a (and therefore b and γ) depends on the actual location of the critical point along the glass transition lines. So this provide us with the possibility of carefully checking the peculiar MCT prediction connecting the exponents of the critical decay law and the relaxation time near the transition over a wide range of parameters. In particular, when the point $(v_1^*, v_2^*) = (1, 1)$ separating the discontinuous and continuous transition is approached, a tends to vanish. Near this glass singularity, which is also called a degenerate A_3 point, the power-law behavior turns into logarithmic relaxation.

III. FACILITATED SPIN SYSTEMS AND BOOTSTRAP PERCOLATION ON BETHE LATTICE

The basic assumption of the dynamical facilitation approach is that, on a suitable coarse-grained lengthscale, one can model the structure of a liquid by an assembly of higher/lower density mesoscopic cells with *no* energetic interaction. A binary spin variable is assigned to every cell depending on its solid- or liquid-like structure. The next crucial step is to postulate that there exists a timescale over which the effective microscopic dynamics can be mapped onto a "simple" form: local changes in cells structure occur if and only if there is a sufficiently large number, say f, of nearby liquid-like cells (f is called the facilitation parameter). The latter assumption is admittedly quite remote from the actual liquid dynamics, and indeed very difficult to derive by analytical means. Nevertheless, it can be justified on physical grounds: it mimics the cage effect and gives rise to a large variety of remarkable, and sometimes unexpected, glassy features, even if the thermodynamics is completely trivial. They include stretched exponential relaxation, super-Arrhenius equilibration time, physical aging, effective temperature, exponential multitude of blocked states, dynamical heterogeneity, etc.

Facilitated spin models consist of N non-interacting spins $\sigma_i = \pm 1$, $i = 1, \ldots, N$ with Hamiltonian

$$\mathcal{H} = -\frac{h}{2} \sum_{i=1}^{N} \sigma_i. \tag{9}$$

Spins evolve according to a Metropolis-like dynamics: at each time step a randomly chosen spin is flipped with transition probability:

$$w(\sigma_i \to -\sigma_i) = \min\left\{1, \mathrm{e}^{-h\sigma_i/k_\mathrm{B}T}\right\}, \tag{10}$$

if and only if at least f of its z neighboring spins are in the state -1. When the temperature T is low enough, the fraction of -1 spins is exponentially small, $\mathrm{e}^{-h/k_\mathrm{B}T}$, therefore spin flipping is rare and sluggish relaxation ensues. We consider a Bethe lattice with fixed connectivity, specifically, a regular k-graph with coordination number $z = k + 1$: besides one branch going down, each node has further k branches going up. The tree-like, local structure of the Bethe lattice allows for some exact calculations concerning the asymptotic dynamics. Let us call B the probability that, without taking advantage of the configuration on the bottom, the spin σ_i is in, or can be brought to, the state –1 by only rearranging the sites above it. B verifies the fixed-point equation:

$$B = (1 - p) + p \sum_{i=0}^{k-f} \binom{k}{i} B^{k-i}(1 - B)^i, \tag{11}$$

where p is the probability that the spin is $+1$ in thermal equilibrium, i.e.:

$$p = \frac{1}{1 + \mathrm{e}^{-1/T}}, \tag{12}$$

where we set $h/k_\mathrm{B} = 1$ hereafter. Equation (11) is closely related to that of bootstrap percolation (BP),[43,47] a problem that is known to emerge in a wide variety of contexts (for a review, see Refs. 48 and 49). In BP every lattice site is first occupied by a particle at random with probability p. Then, one randomly removes particles which have less than m neighbors. Iterating this procedure leads to two possible asymptotic results.[47] If the initial particle density is larger than a threshold p_c there is an infinite cluster of particles that survives the culling procedure, whereas for $p < p_c$ the density of residual particles is zero. In Ref. 47 it has been shown that the probability $1 - B$ that a particle is blocked because it has at least m neighboring particles above it which are blocked (without taking advantage of vacancies below) satisfies the self-consistent Eq. (11). By exploiting the relation with the BP one can characterize the dynamics on a Bethe lattice. There are three qualitatively distinct cases that we now discuss.

A. Noncooperative dynamics

For $f = 1$, any spin only needs one nearby down-spin to flip and the dynamics is called *noncooperative*. Equation (11) becomes

$$1 - B = p(1 - B), \tag{13}$$

obviously implying that there is only the solution $B = 1$ for any p, i.e., with probability one each spin can be brought into the up-state through a finite number of allowed spin-flips. One can see that relaxation dynamics has a single-step form with an Arrhenius equilibration time at any temperature. Thus, the noncooperative case may be useful for modelling *strong* glasses. For this reason it will not be considered here. For more complex forms of glassy dynamics we need local relaxation events involving two or more facilitating (down) spins, i.e., a cooperative dynamics.

B. Cooperative dynamics

1. Continuous transition

For $f = k$ or $k + 1$ there is an additional solution, with $B < 1$, of Eq. (11) which is obtained when p is large enough. The transition to this regime is *continuous*, because for arbitrary small $1 - B$, Eq. (11) becomes

$$1 - B = p \binom{k}{f-1} (1 - B)^{k-f+1} + \ldots, \tag{14}$$

which implies $p_c = 1/k$ for either $f = k$ or $k + 1$. Notice that in the later case, the equation has the exact same form as for $f = k$. In fact, these cases are completely equivalent to conventional percolation,[47] and for this reason, near p_c the incipient cluster of permanently frozen spins (i.e., spins unable to flip because surrounded by more than f neighboring up spins) has a *fractal* structure. The facilitated spin dynamics of these systems has never been explored to our knowledge. We notice that the critical temperature in this case is negative $1/T_c = -\ln(k - 1)$. This means that in order to study relaxation dynamics one must start with initial configurations having a majority of down spins.

2. Discontinuous transition

For $1 < f < k$ the power of $1 - B$ on the right and left hand side of Eq. (14) are different and therefore only a *discontinuous* transition – at a critical value p_c that depends on k and f – is possible. This transition is characterized by a square root singularity coming from low temperatures and is rather peculiar as it produces an unusual *mixed* or *hybrid* behavior: the fraction of frozen spins jumps from zero to a finite value, with divergent fluctuations as in critical phenomena. This is much similar to the behavior of the non-ergodicity parameter in MCT and this form of dynamical arrest corresponds to the sudden emergence of a giant cluster of frozen spins with *compact* structure. The geometric origin of this behavior has been understood quite in detail as being related to the divergence of the size of *corona* clusters near the transition.[50,51] Several results,[42] including those related to large scale cooperative rearrangements responsible for slow dynamics,[52] and the TAP-like organization of blocked states below the threshold,[43] have already suggested a close analogy with MCT and mean-field disordered systems.

IV. FACILITATED SPIN MIXTURES WITH TUNABLE FACILITATION: EXACT RESULTS

The systems considered so far have a fixed facilitation determined by the integer number f, and so they can exhibit either a discontinuous or a continuous glass transition. In this section we consider a recently introduced class of facilitated spin systems in which the facilitation strength can be smoothly tuned.[44] This is obtained by making the facilitation parameter a lattice site dependent random variable, in close analogy with the random bootstrap percolation problem studied by Branco[53] (see also Refs. 54, 55 for recent developments in the context of complex networks). This means that for every site i the facilitation of the spin σ_i is a random variable generally described by the probability distribution

$$\mathcal{P}(f_i) = \sum_{\ell=0}^{k+1} w_\ell \, \delta_{f_i,\ell}, \tag{15}$$

where the weights $\{w_\ell\}$ controlling the facilitation strength satisfy the condition $0 \le w_\ell \le 1$ and the normalization

$$\sum_{\ell=0}^{k+1} w_\ell = 1. \tag{16}$$

By suitably changing the coefficients $\{w_\ell\}$ one can thus explore a variety of different situations, e.g., the robustness of the glass phase against dilution and, more interestingly, the crossover between the discontinuous and continuous glass transition or the existence of multiple glassy states. We remark that mixtures of particles with different kinetic constraints were first considered in a granular matter context, in the attempt to understand particle segregation phenomena under gravity by a purely dynamical approach.[56–58] Hereafter, we shall denote with $\langle \cdots \rangle_f$ the average over the probability distribution Eq. (15). Following Refs. 43, 47, and 53, we can easily generalize the results presented in Sec. III and evaluate the probability B as:

$$B = 1 - p + p \left\langle \sum_{n=0}^{k-f} \binom{k}{n} B^{k-n} (1 - B)^n \right\rangle_f. \tag{17}$$

As we have already anticipated, the precise nature of the glass transition depends on the behavior of the fraction of permanently frozen spins that, in this framework, can be exactly computed from B as follows:

$$\Phi = \left\langle p \sum_{n=0}^{f-1} \binom{z}{n} B^n (1 - B)^{z-n} + (1 - p) \sum_{n=0}^{f-1} \binom{z}{n} (1 - h)^n h^{z-n} \right\rangle_f, \tag{18}$$

where

$$h = p \left\langle \sum_{m=0}^{f-2} \binom{z-1}{m} B^m (1 - B)^{z-1-m} \right\rangle_f. \tag{19}$$

The two contributions in Eq. (18) represent the probability that a spin is frozen in the ± 1 state, respectively. In order to evaluate Φ, in fact, one must take into account that in the neighborhood of both up and down spin states, there must be less then f facilitated spins. Let us consider, for clarity, the homogeneous facilitated case (for heterogeneous facilitation, one just needs to further average over the distribution Eq. (15)). To be blocked, an up spin (found with probability p) may have, among its z neighbors, up to $f - 1$ down spins. These neighbors already have one spin up (the main spin) and the probability that each one is facilitated is precisely B. The overall contribution of all permutations is thus given by the first term in the above equation. When the main spin is down (with probability $1 - p$), we write a term similar to the first one, but replacing B with $1 - h$. h is the probability of a neighbor of the main spin (that is down) being up (with probability

p) and blocked (because beyond the main spin, we consider the possibility of only $f-2$ further down spins). Notice that now to evaluate h we consider the possible permutations of $f-2$ down spins among the $z-1$ neighbors. When the facilitation is no longer homogeneous, we should average both Φ and h over the distribution $\mathcal{P}(f_i)$.

The calculation of the phase diagram and the fraction of frozen spins for different types of mixtures on a Bethe lattice with $z=4$ is detailed in the Appendix. Here, we shall focus on a ternary mixture with facilitations f_i chosen from the probability distribution

$$\mathcal{P}(f_i) = (1-q)\,\delta_{f_i,k-1} + (q-r)\,\delta_{f_i,k} + r\,\delta_{f_i,k+1}, \qquad (20)$$

with $0 \le r \le q \le 1$. The phase diagram for a Bethe lattice with $z=4$ is depicted in Fig. 1, and comprises two glass transition lines, of discontinuous and continuous nature, given, respectively, by

$$\frac{1}{T_c(q)} = \begin{cases} \ln(8-12q), & 0 \le q \le \frac{1}{2}; \\ \ln\frac{1}{3q-1}, & \frac{1}{2} \le q < \frac{2}{3}. \end{cases} \qquad (21)$$

The two lines join smoothly at $q=1/2$, corresponding to the dynamical tricritical temperature

$$T_{\text{tric}} = 1/\ln 2. \qquad (22)$$

The critical temperature depends only on the total fraction q of $f=z-1$ and z overconstrained spins, but not on their relative importance r. As expected, the glass transition temperature increases with q since the constraints become stronger and the spins more easily blocked when compared to the pure case $q=0$. Notice that for $q=2/3$ the critical temperature diverges signalling that there always exists a finite fraction of permanently frozen spins at any positive temperature. Of course, the above phase diagram can be formally extended to negative temperature, i.e., for $2/3 < q \le 1$, by contemplating the possibility of having an equilibrium distribution of -1 spins larger than 1/2. The highest temperature is then $-\infty$ and corresponds to a fully ordered spins configuration in the –1 state. This is the initial configuration one has to start with to properly perform simulations of equilibrium dynamics at negative temperature. Such a situation will not be considered here. The precise nature of the two glass transitions in Eq. (21) depends on the behavior of the fraction of permanently frozen spins Φ near T_c which, in the specific case $z=4$, is given in Appendix A 1. The behavior of Φ as a function of the temperature is shown in the inset of Fig. 1, for several values of q and with $r=10^{-3}$. The height of the critical plateau, shown as a dotted line in the figure, decreases as q increases, going to 0 as $q \to 1/2$. We remark that the fraction of frozen spins generally depends on r while the phase diagram does not. For $0 \le q \le 1/2$, Φ jumps to a finite value $\Phi_c = \Phi(T_c)$ on the transition line, meaning that the infinite cluster of frozen spins has a compact structure. This structure turns out to be quite resilient against random inhomogeneities in the facilitation strength, in a rather large range of value of q. The critical exponent β associated to the order parameter Φ is obtained by expanding the above equations in the small parameter $\epsilon = T - T_c$. As

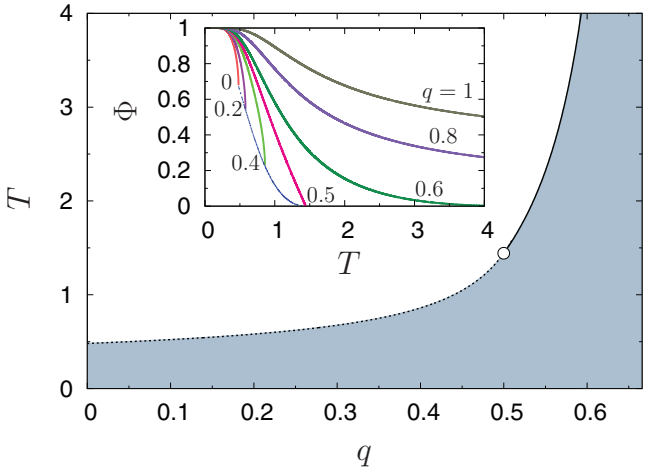

FIG. 1. Phase diagram for $z=4$ and facilitation as in Eq. (20). The dark region is the glassy phase. The dotted/solid line is the hybrid/continuous transition. Inset: Fraction of frozen spins, Eq. (A8), vs temperature for several values of q and $r=10^{-3}$. Below $q=1/2$, Φ jumps to a finite value at the transition which is represented by the dotted line.

expected, when Φ_c has a finite jump, we find $\Phi - \Phi_c \sim \epsilon^\beta$, with $\beta = 1/2$, the typical square-root dependence well known in MCT and in other systems with a hybrid transition. For $1/2 < q < 2/3$ the glass transition changes nature as Φ departs smoothly from zero with a power-law behavior $\Phi \sim \epsilon^\beta$ and the correspondence with standard percolation implies that the giant cluster of frozen spins has a fractal structure. Interestingly, in this case β depends on r: for $r=0$ one has $\beta=2$, while as soon as a negligibly small amount of spins with $f_i = 4$ is introduced into the system, $r>0$, one has $\beta=1$. The robustness of the latter behavior reflects the fact that the mass of the fractal cluster of frozen spins is essentially dominated by the *dangling ends*, that is, those parts of the cluster which are connected to the backbone by a single frozen spin. Only when $r=0$, dangling ends are completely removed from the infinite cluster of frozen spins, and the exponent changes to $\beta = 2$.[53] Hence, the general scenario emerging for an arbitrary ternary mixture is that of two distinct glass transitions with $\beta = 1/2$ (for the discontinuous case), and $\beta = 1$ (for the continuous one). These critical exponents reproduce exactly the MCT results for the F_{12} schematic model.[3] Clearly, it is important to establish how these exponents are attained when the critical line is approached, Also, it is by no means obvious that systems sharing the same order parameter exponents in the glassy phase will also have identical critical dynamical exponents. This type of problems will be addressed in Sec. V.

V. NUMERICAL SIMULATIONS OF A SPIN MIXTURE WITH DISCONTINUOUS AND CONTINUOUS GLASS TRANSITIONS

Since the models we have introduced in Sec. IV are only partially solvable, we now turn to numerical simulation. This will give us the possibility of verifying the power-law behavior of relaxation time with temperature and of critical decay with time and, most importantly, the peculiar prediction of MCT that connects the exponents of these two laws near

the continuous and discontinuous transition line. One obvious advantage of working with facilitated spin models is that one can immediately overcome the problem of the long simulation times needed for thermal equilibration. Moreover, the exact knowledge of both the critical temperature and the arrested part of correlations makes the procedure for estimating power-law exponents much more reliable, as it decreases the number of fitting parameters from three to one. In fact, in real systems, for a given time window, the fitting parameters are correlated: a change of the critical point position in the fit can be compensated, within certain limits, by a change in the power-law exponent. For this reason, one hardly find data, which test the critical decay for more than a two decade time-window. It is also important to remark that testing MCT in systems which are described by a somewhat artificial kinetic rule is particularly interesting because it allows us to probe the degree of universality of MCT prediction beyond the original context (the actual Newtonian or Brownian liquid dynamics) and the closure approximations in which they were originally derived.

A. Persistence

To explore those universal features of relaxation which are relevant for a comparison with MCT we focus on the time evolution of persistence $\phi(t)$, i.e., the probability that a spin has never flipped between times 0 and t. It is a convenient and widely used characterization of the dynamics of facilitated spin systems. The long-time limit of $\phi(t)$ plays the role of the nonergodicity parameter and represents the fraction of permanently frozen spins

$$\Phi = \lim_{t\to\infty} \phi(t). \tag{23}$$

When $\Phi = 0$ the system is a liquid, while for $\Phi > 0$ ergodicity is broken and the system is a glass.

We have been careful enough to disallow initial system configurations with a fraction of permanently frozen spins that would induce dynamical reducibility problems in our simulations (see the discussion in Ref. 39 for details concerning these issues). To this end we have chosen a ternary mixture with a rather negligibly small fraction of spins with $f = 4$, typically $r = 10^{-3}$, and not too large values of q (that is a fraction of spins with $f = 3$). In fact, we observed that the system becomes too overconstrained and reducibility effects begin to appear above $q \simeq 0.55$, at least for the system sizes, $N = 10^5 - 5 \times 10^5$, we have explored in our numerical simulations. At each time unity, called a Monte Carlo step (MCS), N attempts to flip an spin are performed. Simulation results for the persistence $\phi(t)$ are shown in Fig. 2 for various values of q, both above and below the glass transition line $T_c(q)$. We see that above $T_c(q)$, every spin is able to flip so that the long-time limit of persistence is zero, confirming theoretical expectations and the absence of dynamical reducibility effects. Whereas for temperatures inside the glassy phase, $T < T_c(q)$, ergodicity is broken and the persistence attains a finite plateau which is in excellent agreement with the value of Φ analytically computed in Eq. (A8). We also observe that the height of the critical plateau Φ_c (shown as a dotted line in the figure), which is finite for $q < 1/2$, moves towards zero as q approaches 1/2, and remains zero above it. In Sec. IV we have calculated how this Φ_c is approached when $T \to T_c(q)$ and we now compare the exact results with the numerical observations.

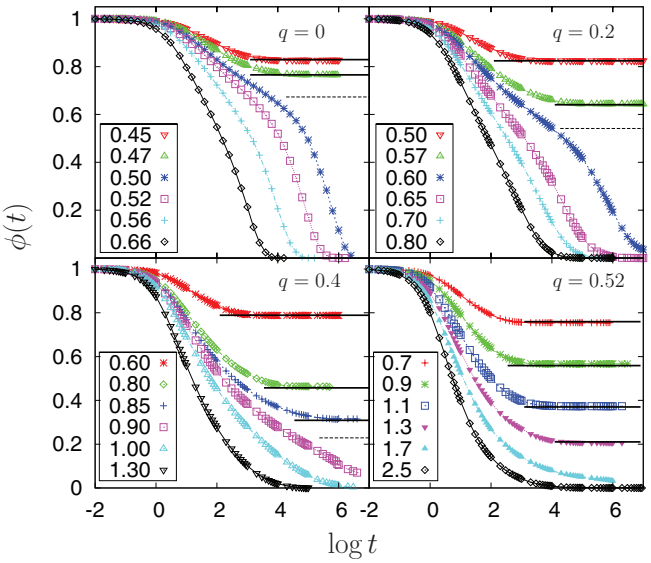

FIG. 2. Persistence vs time for several values of q both in the discontinuous ($q = 0$, 0.2, and 0.4) and the continuous region (0.52) of the phase diagram, Fig. 1, for $r = 10^{-3}$ and several temperatures, either above and below $T_c(q)$. The solid black lines show the theoretical prediction, Eq. (A8), for the plateau heights for $T < T_c(q)$ while the dotted ones signal the critical plateau at $T = T_c(q)$, $q < 1/2$. For temperatures above the transition, the long time value of the persistence is zero.

In the main panel of Fig. 3 we show the behavior of $\Phi(T)$ for small values of r, as described before. The simulations are able to correctly detect the long term plateau as long as it is not too low, otherwise the time to attain it is exceedingly large and beyond our current

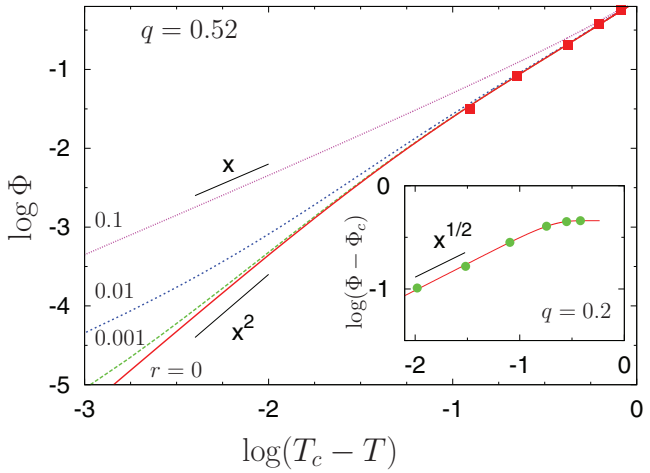

FIG. 3. Asymptotic fraction of blocked spins Φ (plateau height) as the temperature approaches T_c for several values of r and $q = 0.52$ in the continuous region of the phase diagram. Points are the result of simulations while the lines are from Eq. (A8). The relevant temperature interval, in which $\Phi \sim \epsilon^{-1}$, is not accessible in our numerical simulation when $r \neq 0$. Inset: The same for $q = 0.2$ for which the transition is discontinuous (notice the different labels in the y-axis).

computation capabilities. Indeed, the lowest point for which Φ was measured in Fig. 3 corresponds to almost 10^{-2}, that is way before the beginning of the crossover to a linear behavior. The linear in ϵ long-term behavior manifests itself at a much smaller scale, not accessible in our simulation. On the other hand, in the region where the simulation was actually performed, the points are indistinguishable from the $r = 0$ case and closer to the ϵ^2 law. Only when $\Phi(t)$ attains a value of the order of r, and after an exceedingly long crossover, the correct ϵ behavior is observed. It should be noticed that larger values of r could diminish these strong preasymptotic effects, at the expenses of increasing dynamical reducibility effects. This effect could be at the origin of the discrepancy with the value of the measured exponent near the continuous liquid-glass transition.[59] For the discontinuous liquid-glass transition instead we find that the square-root anomaly is very well verified.

B. Relaxation times and critical decay exponents

By measuring $\phi(t)$ at various T and q, see Fig. 2, one can extract more quantitative information that will be useful to check important typical signatures of MCT. When $q < 1/2$, on approaching $T_c(q)$ from the liquid side, the persistence $\phi(t)$ presents the characteristic two-step relaxation form and we can reasonably estimate the characteristic times as follows:

$$\tau = \int_0^\infty \phi(t)dt, \qquad \tau_\beta = \int_0^{t_c} \phi(t)dt, \tag{24}$$

where t_c is the time at which persistence crosses the critical plateau, $\phi(t_c) = \Phi_c$. Notice, that according to these definitions, τ coincides with τ_β when $\Phi_c = 0$ (i.e., when the glass transition is continuous).

With these definitions of relaxation times, and after rescaling time by the structural relaxation time τ, we can check the existence of universal scaling properties of persistence in the late α-regime. For times in the range over which $\phi(t) < \Phi_c$, we find a nice data collapse of persistence function once the time is measured in units of τ, see Fig. 4. The range over which this time-temperature superposition principle holds shrinks when $q \to 1/2^-$ (and so $\Phi_c \to 0$), and consequently no simple scaling form of relaxation data at various temperature can be found in this limit. The scaling function is well fitted by a Kohlrausch-Williams-Watts stretched exponential function with an exponent that decreases as $q \to 1/2$.

To make a more stringent test of MCT we now examine in detail the critical dynamics on the glass transition lines, for which MCT predicts distinctive patterns of universal critical behavior. When the system is relaxing exactly at the critical temperature $T_c(q)$, MCT predicts a power law decay:

$$\phi(t, T_c(q)) - \Phi_c(q) \sim t^{-a(q)}, \tag{25}$$

irrespective of whether $\Phi_c(q)$ is finite or zero. The main panel of Fig. 5 shows that this power law behavior is very well obeyed, either above and below $q = 1/2$. Slightly above or below T_c, the deviations from the power law are also predicted by MCT, Fig. 6: for temperatures equally distant from T_c, the departure from the critical power law is symmetric[12] and starts roughly at the same time. Accordingly with MCT,

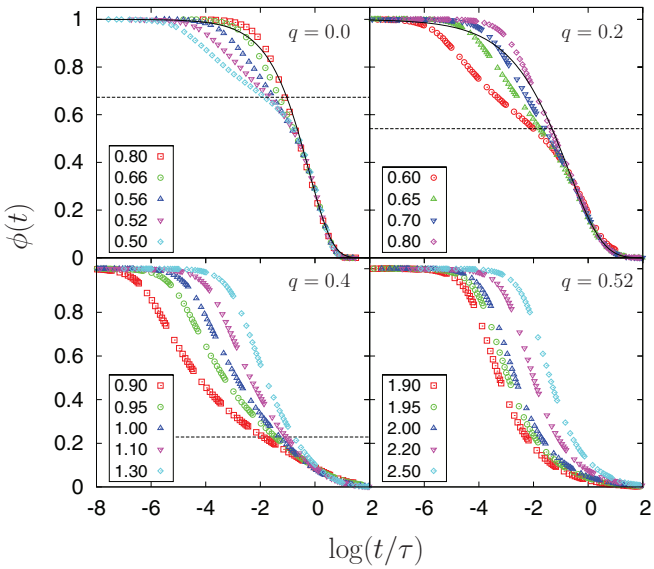

FIG. 4. Data collapse of persistence data for several values of q versus the rescaled time, t/τ, where τ is the characteristic time associated with the α relaxation. We obtain a good collapse for data such that $\phi(t) < \Phi_c$ and, as $\Phi_c \to 0$ when $q \to 1/2$, the collapse region decreases as well, disappearing above the dynamical tricritical point. The collapsed region is well described by a KWW stretched exponential, shown as solid lines for $q = 0$ and 0.2. The stretched exponent is 0.5 for $q = 0$ and 0.35 for $q = 0.2$.

the exponent $a(q)$ is intimately related, in a way that depends on the nature of the glass transition, to the power-law exponent describing the divergence of the characteristic time τ_β as the plateau at Φ_c is approached (the so-called β-relaxation regime): when temperature gets closer to $T_c(q)$ one has $\tau_\beta \sim \epsilon^{-1/2a(q)}$ for the discontinuous transition, and $\tau_\beta \sim \epsilon^{-1/a(q)}$ for the continuous one. These two distinct behaviors are tested in the inset of Fig. 5. Notice that the straight lines in the inset for describing the data of β-relaxation time, measured with Eq. (24), are not fitting functions but use the exponent a of the critical decay law measured in the main panel. The estimated

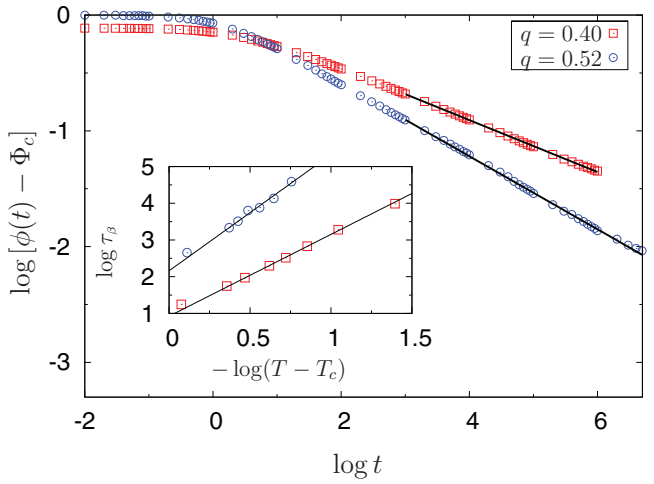

FIG. 5. Equilibrium relaxation at criticality for discontinuous ($q = 0.4$, $T_c \simeq 0.86$) and continuous ($q = 0.52$, $T_c \simeq 1.72$) ergodic-nonergodic transition: solid lines in the main panels are power-law fits with exponents $a \simeq 0.23$ and 0.31, respectively. Inset: β-relaxation time τ_β vs temperature difference $T - T_c$. The solid lines are power-law functions with exponents $1/2a$ and $1/a$, where the value of a is obtained by the fits in the main panel.

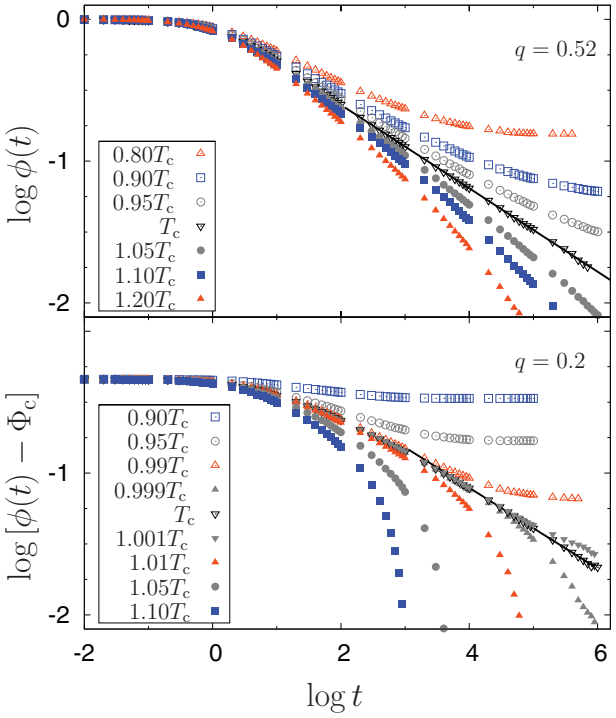

FIG. 6. Symmetric departure from the critical power law behavior for curves at temperatures equidistant from T_c, for $q = 0.52$. The closer the temperature gets to T_c, the more symmetrical the curves become and the longer it takes to depart from the critical power law. An analogous behavior is observed for $q = 0.2$ as well.

τ behaves as a power-law of ϵ near T_c and, more importantly, the exponents perfectly agree with MCT, for both the hybrid and continuous glass transition. In Fig. 7 we collect the results of these two independent ways to measure the exponent a, for several values of q. They show excellent agreement. It is also interesting to observe that the exponent a decreases when $q \to 1/2$, from both side of the continuous and discontinuous region. Although we were able to fit data of $a(q)$ with a function that vanishes at $q = 1/2$, we were not able to approach this

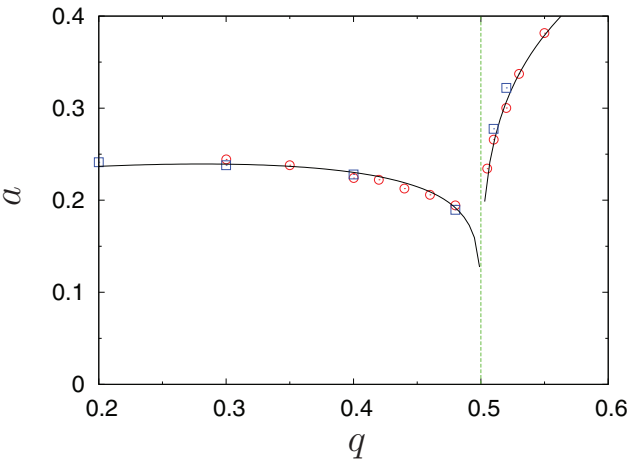

FIG. 7. Exponent a obtained from the critical relaxation (circles) and from the characteristic time as the critical line is approached from above (squares). The solid lines are power-law fits that vanish as $q \to 1/2$, consistently with a logarithmic relaxation at that point.

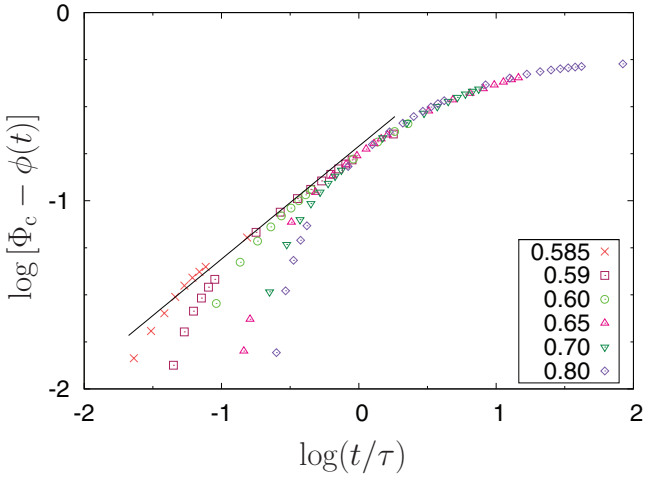

FIG. 8. Estimate of the exponent b for $q = 0.2$ and $r = 10^{-3}$. For this value of q, $T_c \simeq 0.58$ and one obtains $\gamma \simeq 2.81$, $a \simeq 0.25$ and, using Eq. (7), $b \simeq 0.61$. This predicted value is in very good agreement with the simulation, as shown by the solid line whose slope is 0.61.

value of the exponent from the persistence at $q = 1/2$, at least with the sizes and times available to our computer simulation.

Finally, we test the relation among the various exponents a, b, and γ. For $q = 0.2$, the critical temperature is $T_c \simeq 0.58$, and we obtain $\gamma \simeq 2.81$ and $a \simeq 0.25$ from the measure of τ and τ_β, respectively, Eq. (6). Thus, Eq. (7) gives $b = (2\gamma - 1/a)^{-1} \simeq 0.61$. Plugging this value of b in Eq. (5), we can compare the von Schweidler's law against the numerical data of simulations, Fig. 8. We observe that in the late β relaxation regime the agreement between the two is quite good.

VI. DISCUSSION AND CONCLUSIONS

We have extended the Fredrickson-Andersen facilitation approach to glassy dynamics by introducing spin mixtures with different types of facilitation rules.[44] Depending on the cooperative nature of the facilitation, they exhibit a crossover from a discontinuous to a continuous glass transition. We have carefully tested by numerical simulation this approach on a Bethe lattice by analyzing the equilibrium dynamics near the liquid-glass transition lines. The results are fully consistent with predictions of MCT and suggest that the cooperative facilitation approach is the simplest microscopic on lattice realization of MCT. The existence of such a correspondence is by no means obvious because MCT is formulated for many-particle systems obeying Newtonian or Brownian dynamics, while the facilitation approach concerns particles on lattice obeying an abstract—though physically motivated—kinetic rule. The close relation between MCT and systems with quenched disorder,[21,22] suggests in fact that the dynamical facilitation description of glassy dynamics is not in conflict with the RFOT approach. The reason underlying this correspondence (that in a special case can be exactly proved[46]) seems to be quite general,[45] even though it is not trivial to find the explicit expression of the mapping. To explore further the correspondence between facilitated and disordered systems it would be certainly relevant to investigate the possibility of inferring the exponent λ, Eq. (7), from the MCT kernel or from

the associated "free energy" as proposed in Refs. 60 and 61. Also, it is interesting to observe that, while MCT struggles in the real space high dimensional (mean-field) limit,[29,30] no such problem is observed in the Bethe lattice.

The nature of the higher-order glass singularity and other peculiar dynamical features we observed is primarily controlled by the underlying bootstrap percolation process describing the formation of a spanning cluster of frozen spins. The geometric structure of this cluster can be fractal or compact depending on the nature of the cooperative dynamics. The connection with the bootstrap percolation problem can provide some clues on the fate of dynamical glass transition in finite spatial dimensions. Although we do not undertake this delicate task here, we mention that the existence of facilitated models with a dynamical glass transition in finite dimensions,[62–64] naturally suggests that the MCT scenario outlined above for higher-order singularity could be observed also in this circumstance. Also, we expect that the dynamical properties near the continuous and discontinuous liquid-glass transitions are similar to those appearing in the F_{13} scenario (that differs from the F_{12} kernel, Eq. (4), by the presence of a cubic term instead of a quadratic one) because the nature of such transitions is essentially the same in the two schematic models (i.e., a degenerate and generic A_2 singularity).

Although we focused on Bethe lattice with fixed connectivity and random distribution of facilitation, it is worth to remark that one can consider an equivalent variant, in which the Bethe lattice is diluted and the facilitation is uniform.[44] For example, results qualitatively similar to those reported above can be obtained when $f_i = 2$ on every site and the local lattice connectivity z_i is distributed according to

$$\mathcal{P}(z_i) = (1-q)\,\delta_{z_i,4} + (q-r)\,\delta_{z_i,3} + r\,\delta_{z_i,2}. \qquad (26)$$

In this case, less connected sites turn out to have a smaller probability to flip, just as if they were less facilitated. While the former variant has the advantage of being more easily implemented in finite-dimensional systems with fixed coordination number the latter is generally more suitable for systems in which the local mobility does also depend on the geometrically disordered local environment. Thus, the crossover between the two glass transitions is obtained by varying either the local connectivity or the facilitation strength, and corresponds to a passage from bootstrap to standard percolation transition. Whether the fractal cluster of frozen particles can be assimilated to a gel state is an interesting issue that it would be worth to address in a future work.[65,66] Finally, one of the advantages of the present approach is that one can quantify the contribution given by different types of facilitation to the glassy features by studying the dynamics of each species of spins separately. In this respect, it would be interesting to analyze and compare dynamical heterogeneities close to the continuous and discontinuous liquid-glass transition.

ACKNOWLEDGMENTS

We thank D. de Martino and F. Caccioli for their participation in early stages of this work, and W. Götze for clarifications about MCT. J.J.A. is a member of the INCT-Sistemas Complexos and is partially supported by the Brazilian agencies Capes, CNPq, and FAPERGS.

APPENDIX: CALCULATIONS FOR DETERMINING THE PHASE DIAGRAM AND THE FRACTION OF FROZEN SPINS OF FACILITATED SPIN MIXTURES

We report here the detailed calculations to determine the liquid-glass transitions and the fraction of permanently frozen spins for models of facilitated ternary mixtures. With the notation $\ell + m + n$ we denote a ternary mixture composed by spins with facilitation $f = \ell, m$, and n. For the sake of simplicity, we refer to a Bethe lattice with branching ratio $k = z - 1 = 3$, where z is the lattice coordination. We begin with the facilitated spin system we focused in the main text and then consider some other, qualitatively different, representative cases.

1. Ternary mixture 2+3+4

For the ternary mixture 2+3+4 with facilitation distribution

$$\mathcal{P}(f_i) = (1-q)\delta_{f_i,2} + (q-r)\delta_{f_i,3} + r\delta_{f_i,4}, \qquad (A1)$$

the probability that a spin is frozen $1 - B$ obeys the equation:

$$1 - B = p[1 - B^3 - 3(1-q)(1-B)B^2]. \qquad (A2)$$

This equation is always satisfied by $B = 1$, while an additional solution with $B < 1$ is obtained by solving the quadratic equation

$$(3q-2)B^2 + B + 1 - 1/p = 0, \qquad (A3)$$

which gives

$$1 - B = \frac{3(1-2q) + \sqrt{1 - 4(3q-2)(1-1/p)}}{2(2-3q)}. \qquad (A4)$$

The positive sign of the square-root is chosen because B is positive and should decrease as the temperature goes to zero. The continuous transition takes place when the above solution joins the $B = 1$ one. This happens when

$$p_c(q) = \frac{1}{3q}. \qquad (A5)$$

Whereas the vanishing of the square-root argument determines the discontinuous transition:

$$p_c(q) = \frac{8-12q}{9-12q}. \qquad (A6)$$

Using the relation between the temperature T and the probability p

$$\frac{1}{T} = \ln\frac{p}{1-p}, \qquad (A7)$$

one finally gets the dynamical glass transition lines $T_c(q)$ reported in the main text, Eq. (21). The crossover between the continuous and discontinuous transition is obtained when the two expressions of $T_c(q)$ in Eq. (21) becomes equal. This happens at $q = 1/2$ and corresponds to the tricritical temperature, Eq. (22).

The fraction of permanently frozen spins is

$$\Phi = p[(1-B)^3(4+3B) + 6qB^2(1-B)^2 + 4r(1-B)B^3] + (1-p)[h^3(4-3h) + 6qh^2(1-h)^2 + 4rh(1-h)^3], \tag{A8}$$

where B is given by Eq. (A2) and h is

$$h = p(1-B)[(1-B)(1-B+3qB) + 3rB^2]. \tag{A9}$$

2. Ternary mixtures 0+2+3 and 0+2+4

Next we consider the diluted ternary mixtures of type 0+2+3 and 0+2+4. These cases are interesting because they provide us with a phase diagram showing a "tricritical" line separating two glass transition *surfaces*. Let us focus first on the mixture 0+2+3, with

$$\mathcal{P}(f_i) = (1-q)\delta_{f_i,0} + (q-r)\delta_{f_i,2} + r\delta_{f_i,3}. \tag{A10}$$

The probability $1-B$ that a spin is frozen in this case satisfies the equation

$$1 - B = p[q(1-B^3) - (q-r)(1-B)3B^2]. \tag{A11}$$

Beyond the trivial solution $B = 1$ one also finds the extra solution

$$1 - B = \frac{6r - 3q + \sqrt{q^2 - 4(q-1/p)(3r-2q)}}{2(3r-2q)}. \tag{A12}$$

As mentioned before, the continuous transition occurs when the above solution joins the $B = 1$ one, what happens for $p_c = 1/3r$; while the vanishing of the square-root argument in the latter determines the discontinuous transition:

$$p_c(q,r) = \frac{4}{3q}\frac{2q-3r}{3q-4r}. \tag{A13}$$

Using the relation between p and T one finally gets the dynamical glass transition surfaces, $T_c(q,r)$:

$$\frac{1}{T_c(q,r)} = \begin{cases} \ln \dfrac{4(2q-3r)}{12r(1-q)+q(9q-8)}, & \text{(discontinuous);} \\ \ln \dfrac{1}{3r-1}, & \text{(continuous).} \end{cases} \tag{A14}$$

Notice that the continuous transition exists in the interval $1/3 \le r \le 2/3$ and does not depend on q. Interestingly, for any r in the range $1/3 \le r \le 1/2$, there is a dynamical tricritical point whose location in the phase diagram depends on the fraction of free spins. The location of this tricritical line separating the two glass transition surfaces is obtained by setting $q = 2r$, what gives

$$\frac{1}{T_{tric}(q)} = \ln \frac{2}{3q-2}. \tag{A15}$$

Sections of the phase diagram are illustrated in the Fig. 9. Since the equation term related to the spins with $f = 3$ is identical to that of spins with $f = 4$, the phase diagram of the mixtures 0+2+3 and 0+2+4 is just the same. While the related fractions of frozen spins differ: near the continuous transition line they vanish with a different critical exponent, $\Phi \sim \epsilon^\beta$ with $\beta = 2$ for the mixture 0+2+3 and $\beta = 1$ for the 0+2+4 one. The phase diagram structure for mixtures 1+2+3 and 1+2+4 is qualitatively similar.

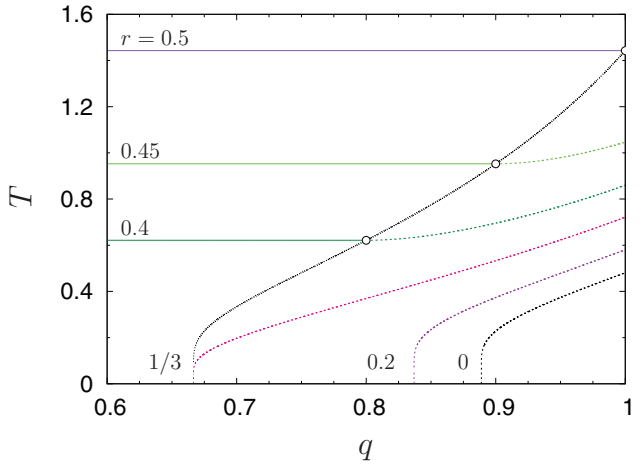

FIG. 9. Phase diagram, temperature T vs fraction of constrained spins q, for the ternary mixture 0+2+3 (and 0+2+4) on a Bethe lattice with $z = 4$ and facilitation as in Eq. (A10). The dotted/full lines are discontinuous/continuous liquid glass transitions for various r. The line passing through the circles is the tricritical line.

We report here only the fraction of frozen spins for the mixture 0+2+3, which is

$$\Phi = pq(1-B)^3(1+3B) + 6pr B^2(1-B)^2 + q(1-p)h^3(4-3h) + 6r(1-p)h^2(1-h)^2, \tag{A16}$$

where B is given by Eq. (A11) and

$$h = p(1-B)^2[3rB + q(1-B)]. \tag{A17}$$

3. Ternary mixtures 0+1+2, 0+1+3 and 0+1+4

Finally, for completeness, we consider the ternary mixtures of type 0+1+2, 0+1+3, and 0+1+4. The calculation proceeds in a manner similar to those outlined above and, as expected, we find only one type of glass transition in these

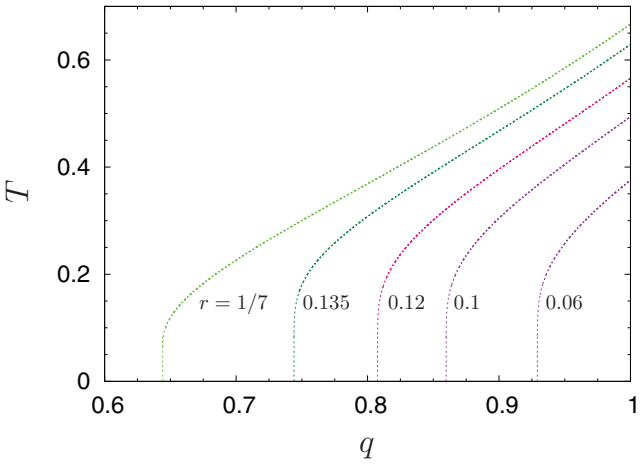

FIG. 10. Phase diagram for the ternary mixtures 0+1+2 on a Bethe lattice with $z = 4$ and facilitation as in Eq. (A18). The glassy region is located below the lines which represent discontinuous liquid-glass transitions for various r.

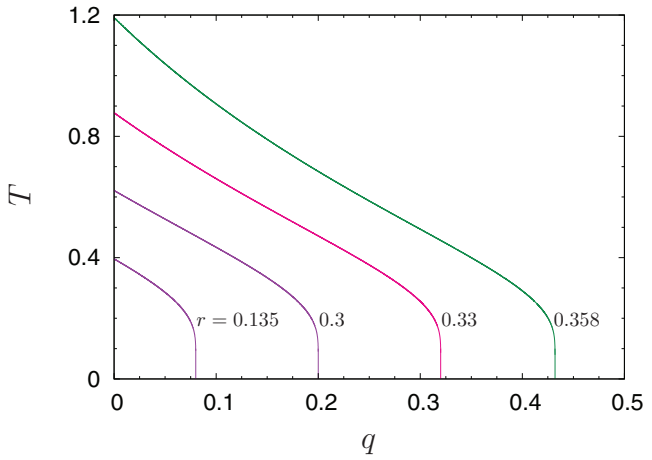

FIG. 11. Phase diagram for the ternary mixture 0+1+3 (and 0+1+4) on a Bethe lattice with $z = 4$ and facilitation as in Eq. (A20). The glassy region is located below the lines which represent continuous liquid-glass transitions for various r.

mixtures. We report here only the expression of their critical lines. For the 0+1+2 mixture with facilitation distributed as

$$\mathcal{P}(f_i) = (1-q)\delta_{f_i,0} + (q-r)\delta_{f_i,1} + r\delta_{f_i,2}, \tag{A18}$$

the glass transition is discontinuous and we get

$$\frac{1}{T_c(q,r)} = -\ln\left[r - 1 + \frac{(2q-3r)^2}{4q-12r}\right]. \tag{A19}$$

For the 0+1+3 mixture with

$$\mathcal{P}(f_i) = (1-q)\delta_{f_i,0} + (q-r)\delta_{f_i,1} + r\delta_{f_i,3}, \tag{A20}$$

we obtain the continuous glass transition

$$\frac{1}{T_c(q,r)} = -\ln(4r-q-1). \tag{A21}$$

The above expression is valid for the case 0+1+4 as well. Sections of the phase diagrams are reported in the Figs. 10 and 11. We notice that the glassy phases generated in the discontinuous and continuous transition are both pretty stable against dilution (or random damage of the underlying lattice). The fraction of free spins can be used in this type of systems as a way to control the plateau height. The phase diagram of binary mixtures can be easily obtained from the previous calculations by setting one of the weights to zero.

[1] K. Binder and W. Kob, *Glassy Materials and Disordered Solids* (World Scientific, Singapore, 2011).
[2] W. Götze and L. Sjögren, Rep. Prog. Phys. **55**, 241 (1992).
[3] W. Götze, *Complex Dynamics of Glass-Forming Liquids* (Oxford University Press, Oxford, 2009).
[4] S. P. Das, Rev. Mod. Phys. **76**, 785 (2004).
[5] D. R. Reichman and P. Charbonneau, J. Stat. Mech. **2005**, P05013.
[6] W. Kob and H. C. Andersen, Phys. Rev. Lett. **73**, 1376 (1994).
[7] W. Kob and H. C. Andersen, Phys. Rev. E **51**, 4626 (1995).
[8] K. Dawson, G. Foffi, M. Fuchs, W. Götze, F. Sciortino, M. Sperl, P. Tartaglia, T. Voigtmann, and E. Zaccarelli, Phys. Rev. E **63**, 011401 (2000).
[9] K. N. Pham, A. M. Puertas, J. Bergenholtz, S. U. Egelhaaf, A. Moussaïd, P. N. Pusey, A. B. Schofield, M. E. Cates, M. Fuchs, and W. C. K. Poon, Science **296**, 104 (2002).
[10] T. Eckert and E. Bartsch, Phys. Rev. Lett. **89**, 125701 (2002).
[11] F. Sciortino and P. Tartaglia, Adv. Phys. **54**, 471 (2005).
[12] V. Krakoviack, Phys. Rev. E **75**, 031503 (2007).
[13] K. Kim, K. Miyazaki, and S. Saito, J. Phys.: Condens. Matter **23**, 234123 (2011).
[14] J. Kurzidim, D. Coslovich, and G. Kahl, J. Phys.: Condens. Matter **23**, 234122 (2011).
[15] E. Leutheusser, Phys. Rev. A **29**, 2765 (1984).
[16] U. Bengtzelius, W. Götze, and A. Sjölander, J. Phys. C **17**, 5915 (1984).
[17] T. R. Kirkpatrick, Phys. Rev. A **31**, 939 (1985).
[18] A. Montanari and G. Semerjian, J. Stat. Phys. **124**, 103 (2006).
[19] E. Siggia, Phys. Rev. A **32**, 3135 (1985).
[20] S. P. Das, G. F. Mazenko, S. Ramaswamy, and J. Toner, Phys. Rev. A **32**, 3139 (1985).
[21] T. R. Kirkpatrick and P. Wolynes, Phys. Rev. A **35**, 3072 (1987).
[22] T. R. Kirkpatrick and D. Thirumalai, Phys. Rev. B **36**, 5388 (1987).
[23] T. R. Kirkpatrick, D. Thirumalai, and P. G. Wolynes, Phys. Rev. A **40**, 1045 (1989).
[24] J.-P. Bouchaud, L. F. Cugliandolo, J. Kurchan, and M. Mézard, Physica A **226**, 243 (1996).
[25] M. Mézard and G. Parisi, J. Chem. Phys. **111**, 1076 (1999).
[26] P. Mayer, K. Miyazaki, and D. R. Reichman, Phys. Rev. Lett. **97**, 095702 (2006).
[27] S. M. Bhattacharyya, B. Bagchi, and P. G. Wolynes, Proc. Natl. Acad. Sci. U.S.A. **105**, 16077 (2008).
[28] A. Andreanov, G. Biroli, and J.-P. Bouchaud, Europhys. Lett. **88**, 16001 (2009).
[29] R. Schilling and B. Schmid, Phys. Rev. Lett. **106**, 049601 (2011).
[30] A. Ikeda and K. Miyazaki, Phys. Rev. Lett. **106**, 049602 (2011).
[31] S. Franz, F. Ricci-Tersenghi, T. Rizzo, and G. Parisi, Eur. Phys. J. E **34**, 102 (2011).
[32] L. F. Cugliandolo and J. Kurchan, Phys. Rev. Lett. **71**, 173 (1993).
[33] L. F. Cugliandolo and J. Kurchan, J. Phys. A **27**, 5749 (1994).
[34] S. Franz and M. Mézard, Europhys. Lett. **26**, 209 (1994).
[35] S. Franz and M. Mézard, Physica A **210**, 48 (1994).
[36] L. F. Cugliandolo, J. Kurchan, and L. Peliti, Phys. Rev. E **55**, 3998 (1997).
[37] L. F. Cugliandolo, J. Phys. A: Math. Theor. **44**, 483001 (2011).
[38] G. H. Fredrickson and H. C. Andersen, Phys. Rev. Lett. **53**, 1244 (1984).
[39] F. Ritort and P. Sollich, Adv. Phys. **52**, 219 (2003).
[40] J. P. Garrahan and D. Chandler, Annu. Rev. Phys. Chem. **61**, 191 (2010).
[41] J. Kurchan, L. Peliti, and M. Sellitto, Europhys. Lett. **39**, 365 (1997).
[42] M. Sellitto, J. Phys.: Condens. Matter **14**, 1455 (2002).
[43] M. Sellitto, G. Biroli, and C. Toninelli, Europhys. Lett. **69**, 496 (2005).
[44] M. Sellitto, D. de Martino, F. Caccioli, and J. J. Arenzon, Phys. Rev. Lett. **105**, 265704 (2010).
[45] M. Sellitto, e-print arXiv:1206.2585.
[46] L. Foini, F. Krzakala, and F. Zamponi, J. Stat. Mech. **2012**, P06013.
[47] J. Chalupa, P. L. Leath, and G. R. Reich, J. Phys. C **12**, L31 (1979).
[48] J. Adler and U. Lev, Braz. J. Phys. **33**, 641 (2003).
[49] P. De Gregorio, A. Lawlor, and K. A. Dawson, in *Encyclopedia of Complexity and Systems Science*, edited by R. A. Meyers (Springer New York, 2009), pp. 608–626.
[50] S. N. Dorogovtsev, A. V. Goltsev, and J. F. F. Mendes, Phys. Rev. Lett. **96**, 040601 (2006).
[51] J. M. Schwarz, A. J. Liu, and L. Q. Chayes, Europhys. Lett. **73**, 560 (2006).
[52] A. Montanari and G. Semerjian, Phys. Rev. Lett. **94**, 247201 (2005).
[53] N. S. Branco, J. Stat. Phys. **70**, 1035 (1993).
[54] G. J. Baxter, S. N. Dorogovtsev, A. V. Goltsev, and J. F. F. Mendes, Phys. Rev. E **82**, 011103 (2010).
[55] D. Cellai, A. Lawlor, K. A. Dawson, and J. P. Gleeson, Phys. Rev. Lett. **107**, 175703 (2011).
[56] M. Sellitto and J. J. Arenzon, Phys. Rev. E **62**, 7793 (2000).
[57] Y. Levin, J. J. Arenzon, and M. Sellitto, Europhys. Lett. **55**, 767 (2001).
[58] H. C. M. Fernandes, J. J. Arenzon, Y. Levin, and M. Sellitto, Physica A **327**, 94 (2003).
[59] A. J. Moreno, S. H. Chong, W. Kob, and F. Sciortino, J. Chem. Phys. **123**, 204505 (2005).
[60] F. Caltagirone, U. Ferrari, L. Leuzzi, G. Parisi, F. Ricci-Tersenghi, and T. Rizzo, Phys. Rev. Lett. **108**, 085702 (2012).
[61] G. Parisi and T. Rizzo, e-print arXiv:1205.3360.
[62] C. Toninelli, G. Biroli, and D. S. Fisher, Phys. Rev. Lett. **96**, 035702 (2006).
[63] M. Jeng and J. M. Schwarz, Phys. Rev. Lett. **98**, 129601 (2007).
[64] H. Ohta and S. Sasa, e-print arXiv:1112.0971.
[65] E. Del Gado, A. Fierro, L. de Arcangelis, and A. Coniglio, Phys. Rev. E **69**, 051103 (2004).
[66] E. Zaccarelli, J. Phys.: Condens. Matter **19**, 323101 (2007).